Temperature-Sensitive and Circadian Oscillators of *Neurospora crassa* Share Components

Suzanne Hunt, Mark Elvin, and Christian Heintzen[1]
Faculty of Life Sciences, University of Manchester, Manchester M13 9PT, United Kingdom

ABSTRACT In *Neurospora crassa*, the interactions between products of the *frequency* (*frq*), *frequency-interacting RNA helicase* (*frh*), *white collar-1* (*wc-1*), and *white collar-2* (*wc-2*) genes establish a molecular circadian clockwork, called the FRQ-WC-Oscillator (FWO), which is required for the generation of molecular and overt circadian rhythmicity. In strains carrying nonfunctional *frq* alleles, circadian rhythms in asexual spore development (conidiation) are abolished in constant conditions, yet conidiation remains rhythmic in temperature cycles. Certain characteristics of these temperature-synchronized rhythms have been attributed to the activity of a FRQ-less oscillator (FLO). The molecular components of this FLO are as yet unknown. To test whether the FLO depends on other circadian clock components, we created a strain that carries deletions in the *frq*, *wc-1*, *wc-2*, and *vivid* (*vvd*) genes. Conidiation in this ΔFWO strain was still synchronized to cyclic temperature programs, but temperature-induced rhythmicity was distinct from that seen in single *frq* knockout strains. These results and other evidence presented indicate that components of the FWO are part of the temperature-induced FLO.

CIRCADIAN clocks are self-sustained, temperature-compensated oscillators that bring temporal organization to living systems on timescales that mimic the 24-hr day. Just as physical and chemical oscillators can lock their frequencies to that of an external periodic force, circadian oscillators can adjust their pace to that of daily light or temperature cycles in a process called entrainment. Entrainment ensures that biological oscillators stay in tune with local time and that a characteristic phase relationship between oscillator and environment is established that directs biological activities to the times of day when they are of highest adaptive value (Bruce 1960; Ouyang *et al.* 1998; Johnson *et al.* 2003; Roenneberg *et al.* 2003; Dodd *et al.* 2005; Price-Lloyd *et al.* 2005; Merrow and Roenneberg 2007).

In the past decades the eukaryotic model organism *Neurospora crassa* has played an important role in the investigation of rhythmic phenomena that bear both circadian and noncircadian characteristics (Roenneberg and Merrow 2001; Lakin-Thomas and Brody 2004; de Paula *et al.* 2007; Heintzen and Liu 2007; Loros *et al.* 2007). In *Neurospora*, circadian rhythms are generated by a network of autoregulatory feedback loops that center on the products of the *frequency* (*frq*), *frq-interacting helicase* (*frh*), and *white-collar* (*wc-1*, *wc-2*) loci (Dunlap 1999; Bell-Pedersen *et al.* 2005; Heintzen and Liu 2007). One of the most easily measured circadian outputs in *Neurospora* is asexual spore development, also known as conidiation. In constant darkness and constant temperature and in the presence of a functional FRQ-WHITE-COLLAR Oscillator (FWO), conidiation occurs with ~22-hr periodicity. In *Neurospora*, the disruption of the FWO leads to a general collapse of molecular and overt circadian rhythmicity. Nevertheless, strains lacking core components of the circadian clock, such as *frq*-less and *wc*-less mutants, can produce rhythms in spore development in certain conditions (Loros and Feldman 1986; Aronson *et al.* 1994; Merrow *et al.* 1999; Lakin-Thomas and Brody 2000; Correa *et al.* 2003; Granshaw *et al.* 2003; Christensen *et al.* 2004; He *et al.* 2005). These observations suggested that other circadian or noncircadian oscillators exist in addition to the FWO. The best studied of these oscillators was first described due to a spontaneously arising rhythm in conidiation in strains carrying the nonfunctional frq^9 allele and is referred to as the canonical FRQ-less oscillator (FLO) (Loros and Feldman 1986; Loros *et al.* 1986; Iwasaki and Dunlap 2000). Later, a robust rhythm in conidiation was discovered

doi: 10.1534/genetics.111.137976
Manuscript received December 19, 2011; accepted for publication February 6, 2012
Available freely online through the author-supported open access option.
Supporting information is available online at http://www.genetics.org/content/suppl/2012/02/23/genetics.111.137976.DC1.
[1]Corresponding author: Faculty of Life Sciences, The University of Manchester, Oxford Road, Manchester M13 9PT, United Kingdom. E-mail: christian.heintzen@manchester.ac.uk

in *frq*-less strains that were exposed to symmetric temperature cycles and interpreted by some as the entrained state of a circadian temperature-induced FLO (Merrow *et al.* 1999). While this interpretation is controversial (Merrow *et al.* 1999; Pregueiro *et al.* 2005; Roenneberg *et al.* 2005), more recent evidence for the existence of other, possibly distinct, FLOs has emerged. For example, the discovery that *clock-controlled gene 16* (*ccg-16*) cycles in a *frq*-less strain, but not in a *wc-1* deletion strain, suggested the existence of a WC-1-dependent FLO (de Paula *et al.* 2006). Furthermore, an investigation into the role of the *period* genes *prd-1*, *prd-2*, *prd-3*, and *prd-4* suggested that they participate in a choline-dependent FLO that was seen in *frq*-null, *choline-1* (*chol-1*) double mutants. (Lakin-Thomas 1998; Li and Lakin-Thomas 2010).

In an attempt to elucidate the molecular basis of the temperature-induced FLO (TI-FLO), we decided to completely abrogate the FWO and study rhythmic spore development in a range of temperature entrainment programs. This approach contrasts with previous studies where the existence of the FLO was inferred from analyzing rhythmicity in strains that lacked just one of several components of the FWO, leaving the possibility that residual or novel network interactions involving the remaining clock components could establish a temperature-responsive oscillator. Here we show that a strain with deletions in *frq*, *wc-1*, *wc-2*, and *vivid* (*vvd*) lacks all traces of entrainment in temperature cycles. In this strain, temperature cycles influence spore development in a manner that resembles a simple stimulus response. Our data suggest that the White Collar Complex (WCC) is important to establish a TI-FLO, *i.e.*, a partially functional oscillatory feedback loop, and that FRQ recruits this loop to make it robust and circadian. The ΔFWO strain should prove useful in future studies that aim to uncover novel oscillators that are independent of the classical circadian oscillator.

Materials and Methods

Strains

All strains and their genotypes that were utilized or generated for this study are listed in Table S1. To create the Δ*wc-2*, *bd*, Δ*vvd*, Δ*frq* Δ*wc-1* strain (ΔFWO), previously described single knockout strains were utilized (Aronson *et al.* 1994; Heintzen *et al.* 2001; Collett *et al.* 2002; Lee *et al.* 2003). A *his-3*, *bd*, Δ*frq*, *A* ^{strain} was crossed to a Δ*vvd*, *bd*, a strain. Δ*vvd*, Δ*frq* double mutants were identified by isolating bright orange (Δ*vvd*), arrhythmic (Δ*frq*) progeny from this cross; putative double mutants were verified by genomic PCR using primers spanning the respective gene loci. Confirmed Δ*vvd*, Δ*frq* double mutants were subsequently crossed to a *his-3*, *bd*, Δ*wc-1*, *A* strain. Δ*vvd*, Δ*frq*, Δ*wc-1* triple mutants were identified by a PCR-based strategy as outlined above using genomic DNA isolated from pale and arrhythmic progeny arising from the cross. A *his-3*, *bd*, Δ*vvd*, Δ*frq*, Δ*wc-1* was thus identified and finally crossed to a Δ*wc-2*, *bd*, Δ*vvd*, *a* strain to obtain the Δ*wc-2*, *bd*, Δ*vvd*, Δ*frq*, Δ*wc-1* (ΔFWO) strain, which was verified by a PCR-based approach as outlined above. The PCR primers used for strain verification were the following: *wc-2*F—5′-CCA AGG TTG TCG AAG AGC-3′; *wc-2*R—5′-GCT AGG TAG TCC CTC TTC ATC-3′; *vvd*F—5′-GAG CTC CAT CTC ATC CTC-3′; *vvd*R—5′-GCC CAA TCG CAG AAT AAG ACG-3′; *frq*F—5′-GTA GCT CTC ATG CGC CCC ACT CTT C-3′; *frq*R—5′-ATT GTC GTC GCT GTC CAT CCG CAC-3′; *wc-1*F—5′-CCC TGT GAT ACC CGA CCC-3′; *wc-1*R—5′-GCT TCC TCC TGA CAT GGT TA-3′; *hph*F—5′-GTG TCA CGT TGC AAG ACC TGC-3′; and *hph*R—5′-CCA GTT GCC TAA ATG AAC CA-3′. The strategy is outlined in Figure 1A and Figure S1. For expression and detection of WC-1 in a ΔFWO or Δ*wc-1* strain, the promoter of the *clock-controlled-1* gene (*ccg-1*) was fused to a MYC-tagged WC-1 ORF. To create Δ*wc-1* (*wc-1*^{myc}), plasmid pMyc-WC-1 (a kind gift from Yi Liu, Southwestern University, Dallas, TX) was electroporated into laboratory strain 104-2 (*his-3*, *bd*, Δ*wc-1*, *A*). To replace the *wc-1* promoter with the *ccg-1* promoter, a *Spe*I site was engineered upstream of the WC-1 start codon by amplifying a PCR fragment using primers WC1P1 (5′-CCC ACT AGT ATG AAC AAC AAC TAC TAC G-3′) and WC1P2 (5′-CGA TCT TGC CCT TTC TAG C-3′). The PCR amplification product replaced a *Spe*I-*Nru*I fragment cut from pWC1myc to yield pWC-1mycSpeI. Finally, a *Not*I-*Spe*I was used to remove the *wc-1* promoter from pWC-1mycSpeI and was replaced by a *Not*I-*Spe*I *ccg-1* promoter fragment obtained from pMF272 (Freitag *et al.* 2004), yielding pSHccg1:WC-1myc. pSHccg1:WC-1myc was electroporated into Δ*wc-2 his-3*; Δ*vvd*; Δ*frq* Δ*wc-1* or *his-3*; Δ*wc-1* to obtain ΔFWO (*ccg1p*:*wc-1*^{myc}) or Δ*wc-1* (*ccg1*p:*wc-1*^{myc}).

Media and growth conditions

All liquid culture and race-tube experiments were carried out in light- and temperature-controlled chambers (SANYO MLR-350 or 351H, Percival Scientific I-36LL or LMS 600A). For standard liquid culture experiments, mycelial disks were inoculated into Erlenmeyer flasks containing 100 ml liquid culture media (1× Vogel's salts, 2% glucose, 50 ng/ml biotin, and 0.17% arginine).

Complete T-cycle experiments: To distinguish between entrained circadian rhythmicity and a driven hourglass-type temperature response, we grew *Neurospora* race-tube cultures in symmetric environmental cycles (T cycles) that consisted of symmetrical temperature cycles between 22° and 30°. For example, a "complete" T-24 cycle consisted of repeating cycles of 12 hr at 22° followed by 12 hr at 30°. Alternatively, a T24 skeleton cycle consisted of 22 hr at 22° followed by 2-hr pulses of 30°.

Incubators were programmed to temperature cycles of different lengths. For each symmetrical T cycle (T16, T24, or T30), the low/high temperature segments were set to 22°/30°. A set of six replicate race-tube cultures was used for each strain and T cycle. Race-tube cultures were held in constant darkness (DD) while exposed to the temperature T cycle and were marked in red safe light at the temperature transitions. Skeleton T-cycle experiments: To replicate the

skeleton-entrainment conditions used by Lakin-Thomas (2006), race-tube cultures were grown in T cycles consisting of 2-hr, 30° temperature pulses given on a background temperature of 22°, thus creating T12, T16, T20, T24, and T30 cycles. Race-tube cultures that were grown in these temperature T cycles were either kept in DD or constant light (LL) (21 μmol $m^{-2} \cdot s^{-1}$) for the duration of the experiment.

Humidity experiments: Race-tube cultures were kept in DD at 22° and exposed to a T24 skeleton humidity T cycle consisting of 2 hr at 60% relative humidity (RH) and 22 hr at 83% RH. With the constant humidity experiments, to keep RH constant at different temperatures, strains were grown on race tubes in complete temperature T12 cycles (6 hr at 22°, 6 hr at 30°) at a constant RH of 60% or without humidity control in which case the temperature change led to corresponding changes in RH between 61% RH at 22° and 38% RH at 30°. Relative humidity was controlled using a temperature- and humidity-controlled growth chamber (MLR-351H, Sanyo), and RH was measured using a built-in, high-molecular membrane-type humidity sensor.

Phase response curve and phase analysis

The idealized phase response curve (PRC) used to predict phases of entrainment in Figure 4 and Figure S3 is based on published data that used 2-hr temperature pulses of 30° on a 25° background temperature to measure their effect on the phase of peaks of conidiation at different times in the circadian cycle (Hunt *et al.* 2007). The data published by Hunt *et al.* (2007) were used to superimpose the idealized PRC using commercially available graphics software (CanvasX, ACD Systems). With respect to this PRC, the peak of conidiation was defined to occur around circadian time 0 (CT0). The "bandwidth" of conidiation peaks was set to ∼3 hr. The PRC was drawn in CanvasX (ACD Systems), and the onsets of the 30° pulse were assumed to elicit an immediate phase response as predicted from the PRC. To obtain stable entrainment, the temperature pulse must strike the PRC at times when the PRC predicts phase shifts (in hours) that equal free-running period (FRP, in hours) − T-cycle length (in hours) (Johnson *et al.* 2004). The FRP of wild-type *Neurospora* was set to 22 hr. Using the idealized PRC, the predicted consequence (from the PRC) of a 2-hr pulse was analyzed by starting at a randomly selected time point at which the pulse strikes the PRC. The predicted phase shift (in hours) caused by this first pulse was determined from the PRC, and the PRC itself shifted accordingly. For each T cycle, this procedure was reiterated until stable entrainment was achieved, which was until the evenly spaced temperature pulses would repeatedly strike the same point (phase) on the PRC; *i.e.*, the PRC was shifted by exactly the amount necessary to be struck at the same time again at all subsequent pulses. From this analysis the locations of the predicted peaks of conidiation were derived. Peaks of conidiation were defined to occur at CT0. Thus, for each T cycle, a standard sine wave with the frequency of the corresponding T-cycle (as predicted for entrainment) was drawn, and peaks were placed as predicted from the PRC model. With the peak thus fixed, all other phase markers were automatically determined and could be used for the modeled phase plots. For the hourglass models, the phases were determined from the model graphs drawn in Canvas. In all cases, onsets and offsets of the modeled rhythms were defined as the up/down transitions through the midline, describing the running average, a procedure that mimicked the settings used for the race-tube analysis described below. Our phase analysis of *Neurospora* cultures followed the procedure reported earlier (Pregueiro *et al.* 2005); *i.e.*, the phase reference points were calculated from race-tube scans that provided an image for subsequent densitometric analysis of the conidiation pattern by the program CHRONO (Roenneberg and Taylor 2000). For calculating the onsets, peaks, offsets, and troughs of conidiation, CHRONO's inbuilt program settings were used. For the calculation of onsets and offsets, the centered moving average of optical density was calculated over a period equalling the T-cycle length. Onset/offset is then defined as the point where the line recording the mean optical density moves up or down through the line describing the running average line. Thus, each individual race tube provided a set of data points for each of the four phase markers. Naturally, the number of data points for each phase marker and race tube varied with T-cycle length, such that, for example, a T16 cycle generally provided more phase markers than a T28 cycle, etc. Race-tube cultures were exposed to the T cycles from the beginning of the experiment, and phase data were calculated only from the third day onward, a time when we deemed the cultures to be stably synchronized. All phase data were exported into Excel (Microsoft) where they were expressed and graphed as hours after the onset of the respective temperature pulses or steps up.

Protein analysis

Protein extracts were obtained as previously described (Garceau *et al.* 1997). For Western blot analysis, 15–50 μg of total protein extract was loaded per lane on 7.5% SDS-PAGE gels. After electrophoresis, proteins were blotted onto Immobilon-P membrane (Millipore) by wet transfer. Membranes were hybridized with anti-MYC antibody (Santa Cruz Biotechnology), and immunodetection was carried out as previously described (Hunt *et al.* 2007).

Results and Discussion

Complete abrogation of the FWO

To create a viable strain in which key components of the FWO are ablated, we deleted the *frq*, *wc-1*, *wc-2*, and *vvd* genes in a single strain (Figure 1A). Henceforth, this Δ*wc-2*; Δ*vvd*; Δ*frq* Δ*wc-1* strain is referred to as the ΔFWO (FRQ-WC-Oscillator knockout) strain. While *vvd* is not essential for rhythmicity in DD in standard laboratory conditions, we decided to delete *vvd* because it participates in a negative feedback loop that represses WCC activity (Heintzen *et al.* 2001; Elvin *et al.*

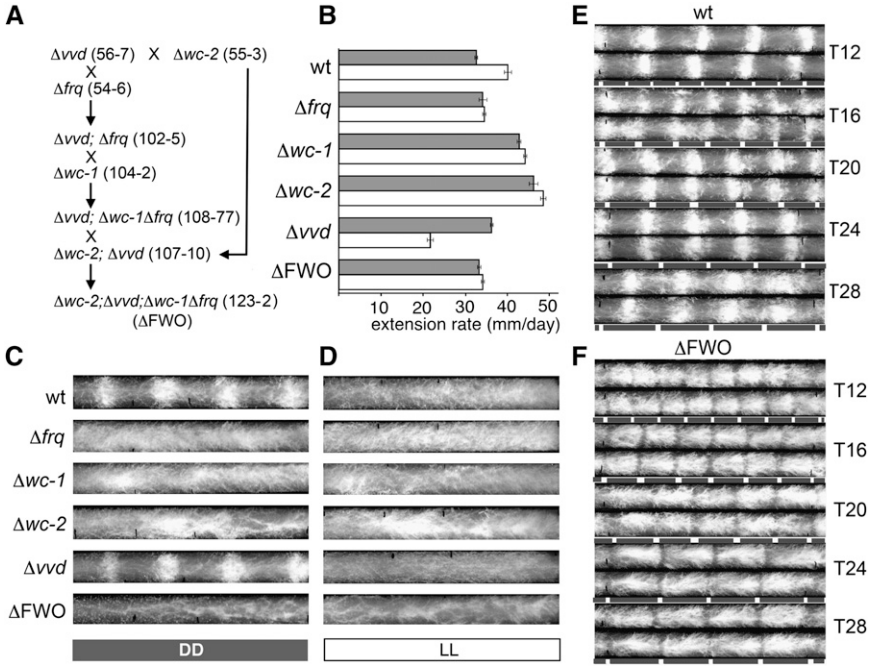

Figure 1 Creation and phenotypic characterization of a ΔFWO strain. (A) Crossing strategy used to generate a ΔFWO strain. All strains carry the *ras-1*^{bd} mutation (not shown). (B) Extension rates of indicated strains in LL (open bars) and DD (shaded bars) at 25°. Error bars indicate ±1 SD. (C and D) Representative race-tube images from strains grown in DD and LL at 25°. (E and F). Race-tube images of wild-type (wt) and ΔFWO strains grown in the indicated temperature skeleton T cycles. The duration of each 28° temperature pulse was 2 hr. Shaded bars: 22°C; open bars: 28°.

2005) and it was possible that this feedback is capable of establishing oscillatory behavior in the absence of FRQ. Moreover, we recently demonstrated that VVD is temperature-regulated (Hunt *et al.* 2007), and, because the TI-FLO is temperature-dependent, an involvement of VVD in temperature entrainment of the FLO was possible. We excluded clock genes whose pleiotropic effects would make a phenotypic analysis or interpretation of rhythmicity in deletion strains impossible, either because they encode essential proteins (FRH, PP1, PP2A) or because they show severe defects in growth and development when ablated (CK1a, CKII, CAMK-1) (Heintzen and Liu 2007). The strategy by which the ΔFWO was obtained and verified is described in *Materials and Methods* and briefly outlined in Figure 1A and Supporting Information, Figure S1. Briefly, starting from a cross of two single deletion strains, we successively generated strains carrying double, triple, and quadruple deletions in which the open reading frames of the respective genes are replaced by the *hph* gene (conferring resistance to hygromycin). Strain 123-2 (see Figure S1) was selected as a representative strain and used in this study as the ΔFWO strain. All strains and their genotypes that were utilized or generated for this study are listed in Table S1.

Growth and conidiation phenotype of a ΔFWO strain

We first characterized the overt phenotype of the ΔFWO strain on race tubes kept at constant temperature (25°) in DD or constant light (LL) alongside the respective single-deletion strains (Figure 1, B–D). The individual deletion strains were included in this analysis as their growth and conidiation phenotypes needed to be analyzed, notwithstanding the fact that *wc-1* levels are low in Δ*frq* strains and *frq* levels are low in Δ*wc* strains, and therefore Δ*wc* strains could be regarded as Δ*frq* strains and vice versa. Under the conditions tested, the ΔFWO mutant showed no obvious growth abnormalities and was overtly arrhythmic in both DD and LL. Extension rates of the ΔFWO mutants in DD were comparable to those of the wild type, while, as previously noted, Δ*wc-1* or Δ*wc-2* knockout strains extended significantly faster in DD; a relatively modest increase in extension rate was also observed in a Δ*vvd* strain when compared to wild type (Figure 1B). Also, extension rates of most strains grown in LL were generally faster than those observed in DD, a phenomenon that could in part be explained by a reduction in aerial hyphae formation and the associated relative increase in lateral growth. It should be noted, however, that growth in LL had a negative effect in a Δ*vvd* strain. This phenotype was similar to the observed growth retardation in LL of an *env* mutant of *Hypocrea jecorina* (in which ENVOY, a putative VVD ortholog, is nonfunctional) and in two *N. crassa vvd* mutants (Schmoll *et al.* 2005; Schneider *et al.* 2009). In conclusion, the ΔFWO mutant strain showed no overtly aberrant growth phenotypes and was deemed a useful tool for the study of oscillatory phenomena that are independent of the circadian FWO oscillator (Figure 1, B–D). It has been suggested that changes in humidity might impact on the conidiation rhythm (Roenneberg *et al.* 2005). We tested this hypothesis in a humidity-controlled chamber. Our results indicate that changes in humidity do not have a measurable effect on overt rhythmicity in temperature cycles (Figure S2).

ΔFWO is temperature-responsive but lacks a FLO

Strains lacking either the *frq* or *wc* genes are arrhythmic when grown in constant darkness under standard laboratory conditions, yet are readily synchronized to temperature cycles (Merrow *et al.* 1999; Pregueiro *et al.* 2005; Roenneberg *et al.*

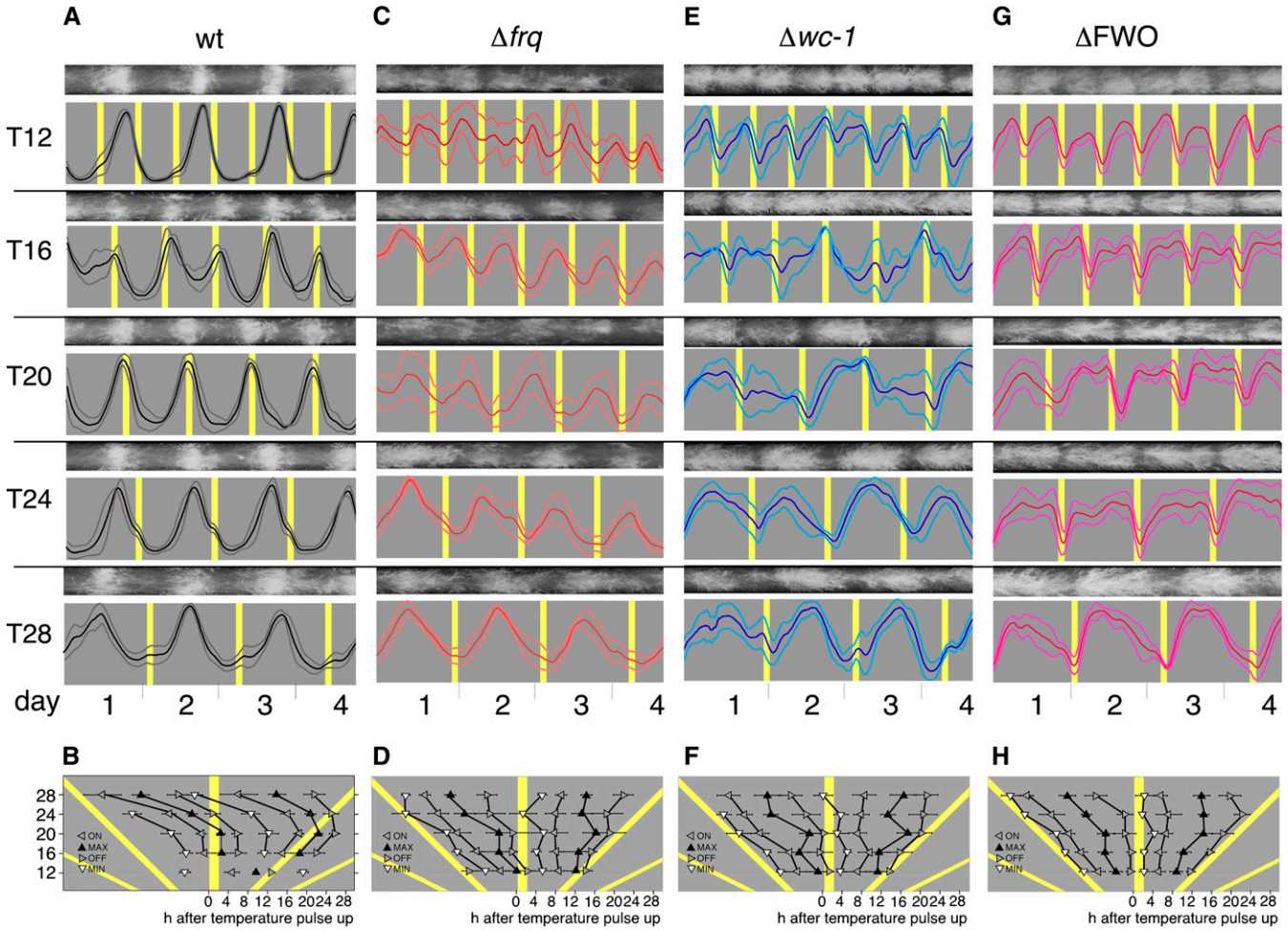

Figure 2 Conidial rhythmicity in skeleton temperature T cycles. Conidiation of wild-type (wt) and clock mutant race-tube cultures grown for 4 days at the indicated temperature skeleton T cycles in constant darkness. (A) Representative race-tube images and densitometric traces for each T cycle of *Neurospora* wild type (wt). Gray: 22°; yellow: 30°. The duration of each 30° temperature pulse is 2 hr. Thick line: mean; thin lines: ±1 SD. (B) Graph showing the dependence of four phase markers on T-cycle length using race-tube traces shown above. The phase markers are onset (ON), offset (OFF), peaks (MAX), and troughs (MIN) of conidiation and recorded in hours following start of temperature pulse (see *Materials and Methods* for more detail). Gray: 22°; yellow: 30°. Error bars indicate ±1 SD. C–H show the same analysis for the indicated clock mutant strains.

2005). A commonly used strategy to distinguish whether rhythms observed under such external "forcing cycles" are controlled by an underlying oscillator or by a simple hourglass-type mechanism involves testing an organism's behavior in a range of symmetric environmental cycles (T cycles). In these experiments, systematic changes in the phase of the observed rhythm are interpreted as oscillator-controlled because the oscillator would complete its cycle before or after the beginning of the next entrainment cue and thus phase-lead or phase-lag the environmental cycle, respectively. In T cycles with sufficiently short frequencies, an oscillator can also "demultiply" to a frequency that is a multiple of the forcing cycle. Systematic phase changes and frequency demultiplication are not expected if the rhythm is generated by a simple stimulus response. In this case, the rhythm should follow the entrainment cue with a fixed delay that is largely independent of cycle length. (Bruce 1960; Pregueiro *et al.* 2005; Roenneberg *et al.* 2005). On the basis of results from previous temperature T-cycle experiments, some groups saw evidence for the action of an entrained FLO in *frq*-less strains (Merrow *et al.* 1999; Roenneberg *et al.* 2005) while others interpreted rhythmicity in a *frq*-less strain as a simple stimulus response to the temperature transitions (Pregueiro *et al.* 2005).

To begin to assess the nature of temperature-induced rhythmicity in ΔFWO strains, we grew ΔFWO strains, alongside the wild-type and single clock mutant strains on race tubes that were exposed to a range of temperature T cycles. In a first set of experiments, we exposed race tube cultures to "skeleton" T cycles to minimize chronic effects of temperature on conidiation and to facilitate comparison of our results with a recent study that had used skeleton T cycles to test temperature-induced rhythms in *Neurospora* single clock mutants (Lakin-Thomas 2006). Race tube cultures of wild type and the various clock mutants were grown in constant darkness at 22° and exposed to regular 2-hr pulses of 30°, thereby establishing T12, T16, T20, T24, and T28

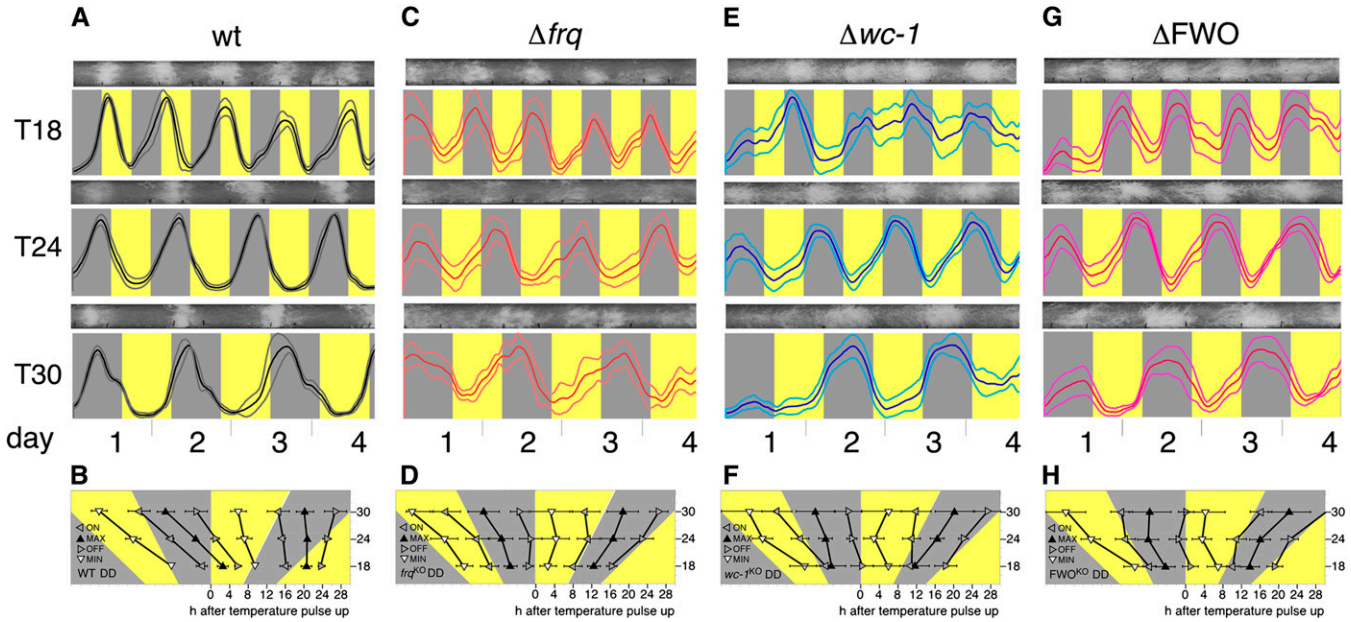

Figure 3 Conidial rhythmicity in complete temperature T cycles. Rhythmic conidiation of wild type (wt) and clock mutant race-tube cultures grown for 4 days at the indicated complete temperature T cycles in constant darkness. (A) Representative race-tube images (top) and densitometric traces (bottom) of *Neurospora* wild-type (wt). Gray shading: 22°; yellow: 30°. Thick line: mean; thin lines: ±1 SD. (B) Graph showing the dependence of four phase markers on T-cycle length using race-tube traces shown above. The phase markers are onset (ON), offset (OFF), peaks (MAX), and troughs (MIN) of conidiation and recorded in hours following start of temperature pulse (see *Materials and Methods* for more detail). Gray: 22°; yellow: 30°. Error bars indicate ±1 SD. C–H show the same analysis for the indicated clock mutant strains.

skeleton cycles (Figure 1, E and F, and Figure 2). For example, a T28 cycle consisted of repeated cycles of 26 hr at 22° followed by 2 hr at 30°. Figure 1, E and F highlight the difference between the temperature response of wild-type and ΔFWO strains when kept in DD and exposed to a range of temperature skeleton T cycles. While both strains were "rhythmic," rhythmicity in a ΔFWO was due to an inhibition of conidiation during the 30° pulse, while conidiation in a wild type showed hallmarks of entrainment as outlined above; *i.e.*, conidiation was not simply following the temperature transitions at fixed time intervals. A detailed analysis of temperature-cycle experiments in DD using wild-type, Δ*frq*, Δ*wc-1*, and ΔFWO strains is shown in Figures 2 and 3. In these experiments, we used either skeleton temperature cycles with 2-hr temperature pulses as described above (Figure 2) or complete temperature T cycles (Figure 3) where half of the repeated cycle was at the lower temperature and the other at the higher temperature. Among the strains tested, only wild-type and Δ*vvd* strains (not shown), *i.e.* strains in which the core circadian FWO is intact, displayed hallmarks of circadian entrainment. Both strains showed systematic changes in their timing of the conidiation (phase) across T cycles and fulfilled the criteria for circadian entrainment as outlined above (see Figure 2, A and B, and Figure 3, A and B). Crucially, in T cycles that are close to half the length (T12) of their natural FRP, both strains "demultiplied"; *i.e.*, they showed peaks of conidiation every 24 rather than every 12 hr (Figure 2A). None of the other strains analyzed, including the ΔFWO, showed any evidence of frequency demultiplication in their conidial rhythms (Figure 2, C–H, and Figure 3, C–H). In all T cycles, the ΔFWO strain appeared to be simply responding to a change in temperature, with conidiation always acutely suppressed at the higher temperature. As a consequence, in a ΔFWO strain, rhythms in temperature-induced conidiation appeared distinctly rectangular. Similar phenotypes were seen in the single *wc-1* and *wc-2* (not shown) knockout strains. In the Δ*frq* strain, high temperature still repressed conidiation but not as acutely as in the ΔFWO, Δ*wc-1*, or Δ*wc-2*; *i.e.*, the bulk of conidiation did not simply occur across the entire cold period, suggesting a residual ability to restrict/influence conidiation in this strain. It is worth noting that in complete entrainment, conidiation at the higher temperatures is not always completely suppressed in clock-less strains and that some degree of anticipation appears to occur (again most pronounced for the Δ*frq* strain). Whether conidiation truly starts before the temperature transition or is simply an acute developmental effect of temperature on already existing, developmentally competent mycelia that are close to the growth front when the temperature transition occurs, we cannot say. These two possibilities could be distinguished by time-lapse analysis of the conidiation rhythm.

The entrainment behavior of the clock in wild type is reflected in the phase plots (Figures 2B and 3B) that show that all phase markers changed as predicted on the basis of the entrainment criteria outlined above, while phase plots for the clock-less strains (Figure 2, D, F, and H; Figure 3, D, F, and H) supported the general impression that rhythmicity

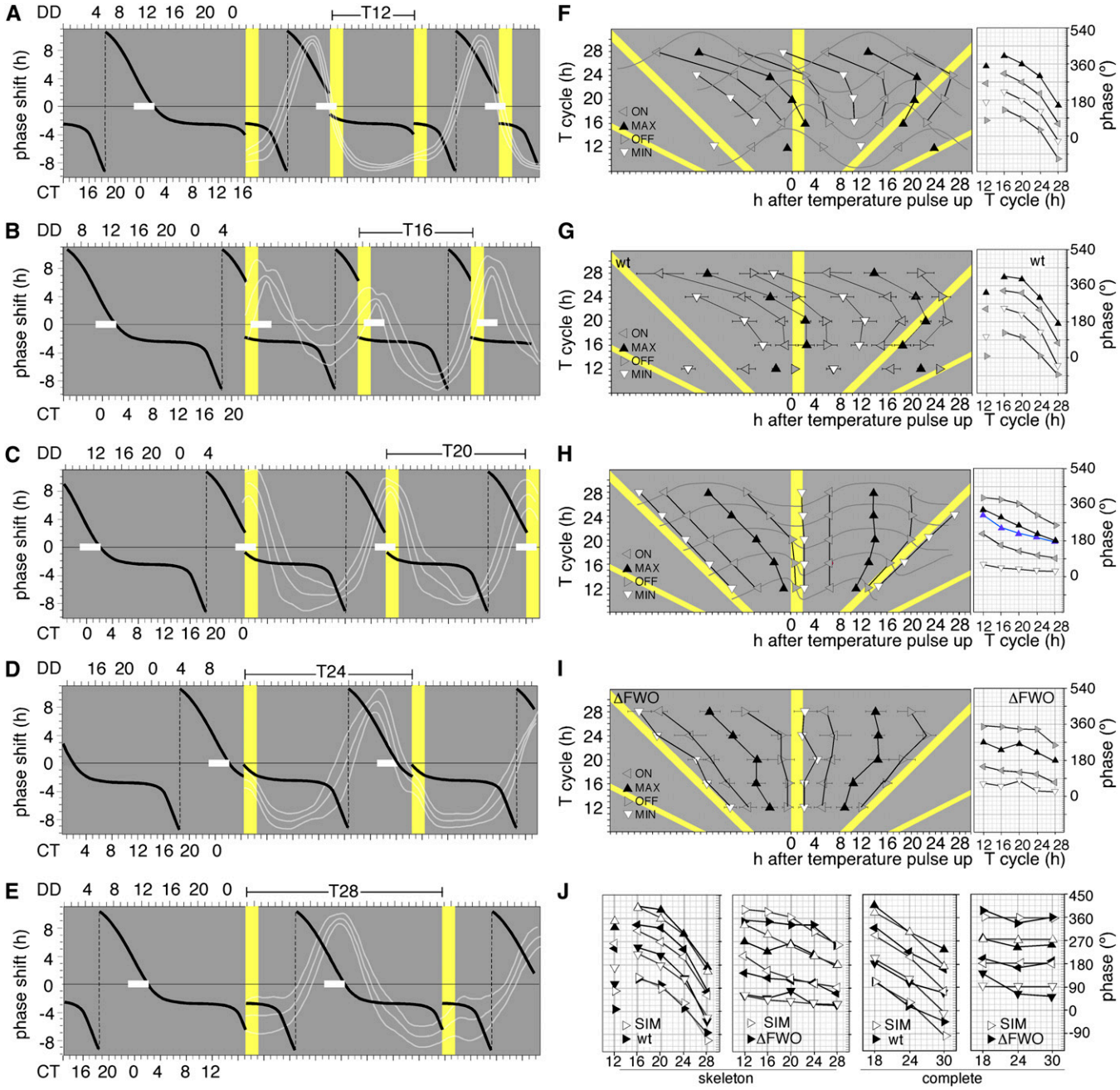

Figure 4 Modeling rhythmicity in temperature T cycles. Prediction of the position of phase markers of entrained and hourglass-type rhythms in *Neurospora* wild-type and circadian clock mutants in skeleton temperature T cycles (A–E) An idealized *Neurospora* phase response curve (PRC, black) illustrates the phase-shifting effects (expressed in hours of phase advances/delays with respect to an unperturbed control) of temperature pulses (2-hr pulses of 30°) given at different circadian times (CT) during the *Neurospora* conidiation cycle. The PRC is based on published data (Hunt *et al.* 2007). The white bars illustrate the location of the peak of conidiation that is fixed with respect to the PRC. Peaks of conidiation are defined here to occur at ~CT0. For entrainment to the various T cycles to occur, a 2-hr 30° temperature pulse will need to strike the PRC at time point(s) where the resulting phase shift is the FRP–T-cycle period. For example, in a T24 cycle and given a wild-type FRP of ~22 hr, the temperature pulse needs to strike at ~CT4 to achieve the required 22–24 hr = −2-h delay. Using the PRC shown, the modeled peaks of conidiation (white bars) are in excellent agreement with the actual experimental data (race-tube traces, white lines). (F and G) Simulated (F) and experimental (G) position of phase markers of conidial rhythms entrained to the shown T cycles. Conidial rhythms were simulated by simple sine waves, and the predicted phase markers are based on the PRC introduced above. Experimental data are derived from phase analysis of the race-tube data shown in Figure 2A. The phase markers shown were recorded in hours following the start of the temperature pulse (yellow) and represent onsets (ON), offsets (OFF), peaks (MAX), and troughs (MIN) of conidiation. The graphs on the right depict the dependence of a phase (expressed in degrees) on the T cycle. For experimental data, only the mean phases are shown. (H and I) Simulated hourglass-type behavior (H) and experimental data for the ΔFWO strain (I) in skeleton T cycles (see Figure 2G). The onset of the temperature pulse has two effects: it resets and it restarts an hourglass-type mechanism. In a T cycle that is shorter than the duration of the stimulus

(*continued*)

is not entrained. With some exceptions, all phase markers align to the temperature transitions. It is notable that standard deviations for each of the phase markers in the clockless strains are large when compared to the wild type, indicating large fluctuations in the position of these phase markers, particularly for Δ*frq*.

Modeling clock wild-type behavior to temperature cycles

To try to better understand the patterns of rhythmicity in wild-type and clock-mutant strains, we attempted to model the positions of the characterized phase markers. In the first approach, we used a previously published PRC as the basis for modeling the times when peaks, troughs, onsets, and offsets of an idealized sinusoidal rhythm in conidiation would be expected to occur within the various T cycles in a clock wild-type strain (Hunt *et al.* 2007) (Figure 4, A–E). The published PRC had used 2-hr 30° temperature pulses on a 25° background and thus was deemed suitable to model entrainment to our skeleton T cycles. There is excellent agreement between the phases of entrainment that are predicted by the PRC and the actual data (white traces in Figure 4, A–E), and this is reflected in the similarities between the predicted and actual phase plots (Figure 4, F and G; compare simulated phases with actual phases in Figure 4J for wild type). Although the PRC used above had limitations with respect to predicting entrainment to complete temperature cycles, we nevertheless obtained good agreement between model and experimental data for the wild type grown in complete T18 and T24 cycles (Figure S3, A and B). These results were consistent with data from Dharmananda (1980) who observed that phase shifts by heat pulses lasting for longer than 40 min and up to 6 hr were similar in magnitude and direction (Dharmananda 1980). Our T18 and T24 data suggested that the heat pulse could be up to 12 hr in length without substantially changing phase-shifting behavior. However, in T30 cycles, the modeled data did not fit the observations and prolonged exposure to high temperatures affected the phase response (Figure S3C). It is likely that this was a combined effect of the temperature up and down transitions as temperature-down transitions were known to produce phase shifts only after prolonged exposure to higher temperatures (Dharmananda 1980). This aside, the modeled and experimental data for wild type were in good agreement (Figure S3, D and E, and Figure 4J: compare simulated with actual phases in complete T cycles for wild type) and fulfilled predictions for entrainment as outlined above.

Modeling ΔFWO behavior to temperature cycles

On the basis of the characteristics of overt rhythmicity of a ΔFWO strain, we used a simple hourglass-type mechanism (Figure 4H) to explain the position of the various phase markers in skeleton T cycles (Figure 4I). The model assumes that the temperature pulse has two effects: (1) it acutely suppresses conidiation at the time of the temperature pulse, and (2) it resets and restarts the development of conidia via an hourglass-type mechanism following the temperature pulse (with the conidiation cycle set to last ~12–14 hr). If, as in shorter T cycles, the next temperature pulse occurs before conidiation has peaked, the pulse will suppress conidiation prematurely. A comparison of Figure 4H and Figure 4I shows that the actual data for ΔFWO fit this model well and that the phase markers between actual and modeled data are in close agreement (Figure 4J). For complete temperature cycles, we assumed a rectangular waveform in which the temperature transitions mark the onsets and offsets of conidiation (Figure S3F). In this model, onsets and offsets of conidiation were restricted to the temperature transitions while peaks and troughs of conidiation occupied the entire half-cycle. The distribution of phase markers in the ΔFWO strain (and those in other clock mutants) was well replicated by this model (Figure S3, F and G; Figure 4J, far right panel). By necessity, in a model that assumes a rectangular waveform for conidiation, the times of peaks and troughs are not restricted to a narrow window of time; *i.e.*, they can be anywhere in the cold or warm part of the cycle, respectively, while onsets and offsets are confined to the temperature transitions. When applied to conidiation, this model predicted that the peak and trough phases are ill-defined because conidiation is not restricted to any particular time in a temperature segment. Nevertheless, peaks and troughs of conidiation can usually be assigned due to biological variations in conidial density during a given temperature segment. This is perhaps best illustrated by looking at the race tube images for the ΔFWO strain shown in Figure 1F; clearly, conidiation occurs across the entire cold segment of the cycle, yet peaks and troughs can be identified due to local variations in conidial density. Given the largely random nature of these events, we predicted that large error bars are associated with these phase makers. Indeed, error bars for peaks and troughs were particularly large (see Figure S3G). Taken together, our T-cycle experiments suggested that a strain lacking key components of the *Neurospora* circadian oscillator, such as the ΔFWO mutant, could only passively respond to temperature cycles (Figures 1F, 2G, and 3G) while a residual ability to influence conidial development was retained in strains in which the *wc* genes were intact, such as in a Δ*frq* strain (Figures 2C and 3C). Although *wc-1* levels are low in Δ*frq* strains, we know that the WCC must be functional in this strain because, for example, the WCC-dependent induction of frq^9 (encoding nonfunctional FRQ protein) and *vvd* transcripts is still seen in Δ*frq* strains (Crosthwaite *et al.* 1997; Heintzen *et al.* 2001).

response (*e.g.*, T20), the next temperature pulse suppresses spore development, and conidiation restarts at the end of the pulse. Phase markers and graphs are as described above. The data highlighted in blue in H are replotted from Lakin-Thomas (2006) and show peaks of conidiation of a *wc-1* mutant strain (see Figure 3A). (J) Comparison of simulated (SIM, open symbols) and experimental (solid symbols, WT and ΔFWO) phase data from skeleton and complete temperature T cycles (also see Figure S3).

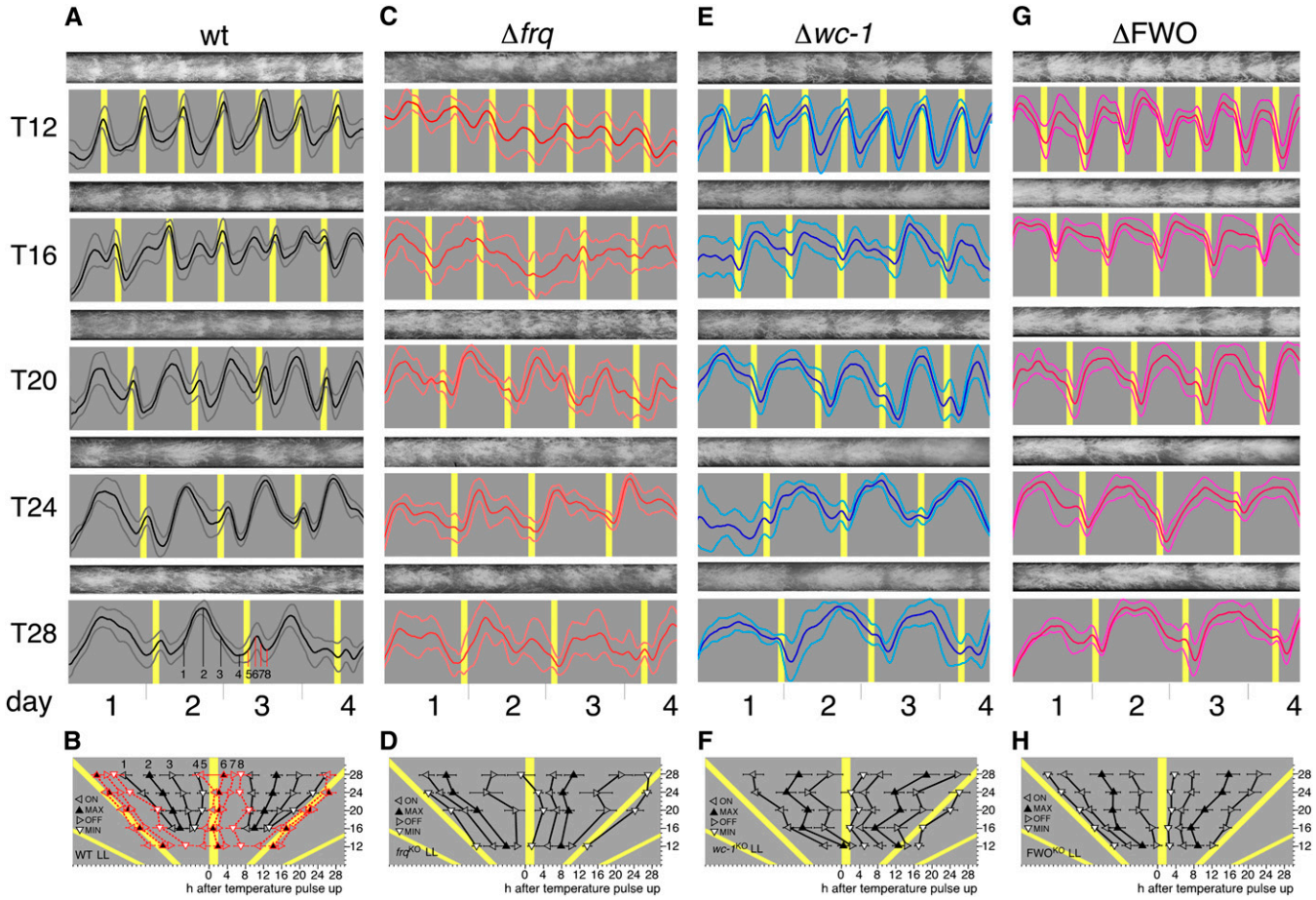

Figure 5 Conidial rhythmicity in skeleton temperature T cycles kept in constant light. Rhythmic conidiation of wild type (wt) and clock mutant race-tube cultures grown for 4 days at the indicated temperature skeleton T cycles in constant light. (A) Representative race-tube images (top) and densitometric traces (bottom) of *Neurospora* wild type (wt). Gray: 22°; yellow: 30°. The duration of each 28° temperature pulse is 2 hr. Thick line: mean; thin lines: ±1 SD. (B) Graph showing the dependence of four phase markers on T-cycle length using race-tube traces shown above. The phase markers are onset (ON), offset (OFF), peaks (MAX), and troughs (MIN) of conidiation and recorded in hours following start of temperature pulse (see *Materials and Methods* for more detail). Because two sets of peaks were easily discernible in the wild type, all of the associated phase markers (1–8, exemplified for T28 in A) were subjected to phase analysis and are shown in black (phase markers 1–4) or red (phase markers 5–8). Gray: 22°; yellow: 30°. Error bars indicate ±1 SD. (C–H) The same analysis for the indicated clock mutant strains. Phase markers were calculated only for the prominent rhythms of conidiation. Note that conidiation in a Δ*frq* grown in a T16 cycle was too erratic to yield reliable data on phase.

The main points that we want to emphasize from these models are the following:

1. A slope in the phase data when plotted against T cycle is not in itself indicative of entrainment, as is sometimes suggested, because a plot of phase markers that are invariant with respect to a T cycle will create a slope when the phase is expressed in degrees (see Figure 4H and Figure 4J, second panel from left). While this slope will indeed be close to 0 when the phase marker is near the temperature transition, it will increase as it moves away from it (compare troughs and peaks of the phase plots in the second panel from left in Figure 4J).
2. An hourglass mechanism does not require that all phase markers (*e.g.*, peaks) are invariant with respect to the temperature pulse. Due to the nature of the modeled hourglass rhythm, the slope of various phase markers from our model is not identical between phase markers; nor is there a linear relationship between the T cycle and the slope of a given phase marker. To illustrate this, we included data from Lakin-Thomas (2006) in Figure 4H (far right panel, blue data points) that show the peaks of conidiation of a *wc-1* mutant strain. These data were interpreted as evidence for entrainment, yet both the slope in the peak phase plots and the differences in the timing of the conidiation peaks are consistent with the depicted hourglass mechanism.
3. Our data suggested that WC-1, WC-2, or the WCC are involved in suppressing conidiation at certain times during cold periods because conidiation covered almost the entire cold period in all strains lacking a functional WCC, such as the ΔFWO, Δ*wc-1*, and Δ*wc-2* mutants (see Figure 2, E and G; Figure 3, E and G; Figure 5, E and G; data not shown), while conidiation in a Δ*frq* strain, *i.e.*, a strain

in which both copies of the *wc* genes are intact, was restricted to certain times during the cold part of the cycle, leading to a more sinusoidal appearance of its conidiation rhythm (Figures 2C, 3C, and 5C).

WCC is required for creating FLO-like rhythms

Recently, de Paula and Colleagues (2006) identified the gene *ccg-16*, which was rhythmically expressed in a *frq*-deletion strain in both DD and LL but was arrhythmic in strains lacking the WCC (de Paula *et al.* 2006). The authors distinguished this FLO from the canonical FLO, and we wondered whether their proposed temperature-sensitive WC-FLO could be responsible for shaping temperature-synchronized rhythmicity in the Δ*frq* strain. We therefore repeated the temperature skeleton regime in an LL background (Figure 5). We reasoned that, if this WCC-dependent FLO controls conidial rhythmicity in the Δ*frq* in DD, rhythmicity should be significantly different when shifted to LL (*i.e.*, to conditions where WCC is induced and activated). This was indeed the case. When comparing LL- *vs.* DD-grown cultures, the timing (phase) of conidiation appeared significantly different in Δ*frq* strains (compare Figure 2, C and D, with Figure 5, C and D). Indeed, a comparison between the times of peaks and troughs of conidiation showed large differences between these phase markers in a Δ*frq* strain, and a detailed statistical analysis (paired *t*-test) for peaks and troughs of conidiation confirmed that these differences are, with one exception, highly significant (paired *t*-test, $P < 0.0001$; see Table S2 for *t*- and *P*-values for all phase markers, T cycles, and strains analyzed). There are also statistically significant differences between LL and DD conditions in Δ*wc-1* and ΔFWO strains for some of the T cycles and phase markers analyzed. However, when compared to the Δ*frq* strain, fewer of the analyzed phase markers show significant phase differences, and, if significant differences existed, they were markedly smaller in a Δ*wc-1* and a ΔFWO strain (in this order). To provide a simple measure of these differences, we summed up all phase differences (between LL and DD conditions) for all T cycles for each strain analyzed (see values in boldface type in Table S2). For example, while the sum of all phase differences seen across the tested T cycles in a Δ*frq* strain is ∼18 hr (for each peak and trough, see Table S2), it is only ∼9 hr in a Δ*wc-1* strain and ∼4 hr in a ΔFWO strain. The small but significant changes in ΔFWO and Δ*wc-1* strains are nevertheless interesting because conidiation in both strains still appears to be somewhat light-sensitive. It is possible that, under these conditions, other putative *Neurospora* photoreceptors reveal their influence on conidiation when the WCC is deleted. For example, the putative *Neurospora* photoreceptors CRY-1 (Froehlich *et al.* 2010), PHY-1, PHY-2 (Froehlich *et al.* 2005), and NOP-1 (Bieszke *et al.* 1999) may influence asexual development by modulating the expression of the conidiation-specific *con-10* gene, as suggested by a recent study (Olmedo *et al.* 2010). In addition or alternatively, light may influence conidiation more indirectly by affecting the levels of reactive oxygen species (ROS) in the cell. Indeed, ROS signaling has been linked to asexual development in Neurospora for some time (Hansberg *et al.* 1993), and more recently, the activity of WCC has been reported to be responsive to and may also influence ROS levels (Yoshida *et al.* 2004; Belden *et al.* 2007). This aside, our results suggested that, in a Δ*frq* strain, residual WCC activity controlled the FLO and that the WCC-FLO identified by de Paula *et al.* (2006) could be identical to the TI-FLO. Indeed, the ability of the *ccg-16* rhythm to be reset by temperature pulses is consistent with our observation that both WC-1 and WC-2 are temperature-regulated. Whether the WCC-FLO and TI-FLO are distinct or identical could be tested in future experiments by assessing whether *ccg-16* levels in strains expressing WC-1 in a ΔFWO strain persist or are abolished,.

As expected, in the presence of the classic light-sensitive FWO, clock-controlled rhythmicity perished as a result of chronic resetting of the FWO in LL (Figure 5, A and B). Consequently, frequency demultiplication in T12 was no longer seen when strains containing the core components of the FWO (*i.e.*, the wild-type and Δ*vvd* strains) were kept in LL while being synchronized to the temperature cycles (Figure 5A, top); peaks in conidiation then occurred during every heat pulse, indicating that conidiation was now simply responding to the temperature pulse. Yet, this simple stimulus response was markedly different from that seen in the clock-less strains in that conidiation in wild-type and Δ*vvd* strains was acutely induced by the temperature pulse in LL rather than inhibited (compare top panels in Figure 5, A, C, E, and G). In the wild type grown in T28 cycles, the phase of conidiation during the cold is similar in both DD- and LL-grown cultures; however, there is a much more pronounced peak in conidiation during the heat pulse in LL (compare bottom panels in Figure 2A and Figure 5A). Similarly, secondary peaks of conidiation appear in the Δ*frq* strain, but they are less pronounced and do not always coincide with the heat pulse (Figure 5C). Because only the wild-type and Δ*vvd* strains contain a fully functional WCC (the WCC is absent in Δ*wc-1*, Δ*wc-2*, and ΔFWO strains and WC-1 levels are very low in a Δ*frq*), we concluded from this set of experiments that the presence of the *white-collar* genes is crucial for shaping overt rhythmicity in cyclic temperature protocols. This conclusion is consistent with the observation that conidiation in both single Δ*wc-1* and Δ*wc-2* mutants closely resembles that of a ΔFWO mutant. Consequently, in the absence of *frq*, the level of activity of WCC determines whether a FLO is established or not. In the absence of sufficient FRQ *and* WCC activity, such as in Δ*wc-1*, Δ*wc-2*, and ΔFWO strains, the circadian oscillator is absent and rhythmicity is simply driven by temperature transitions. In strains with no FRQ but residual WCC activity, a FLO emerges with characteristics that are intermediate between a robust oscillator and a driven hourglass. Thus, only the strains that have both sufficient FRQ and WCC activity, such as is present in wild-type and the Δ*vvd* mutant, have an entrained circadian clock.

The observation that WC-1 levels are low in a Δ*wc-2* strain (Crosthwaite *et al.* 1997) while WC-2 levels are

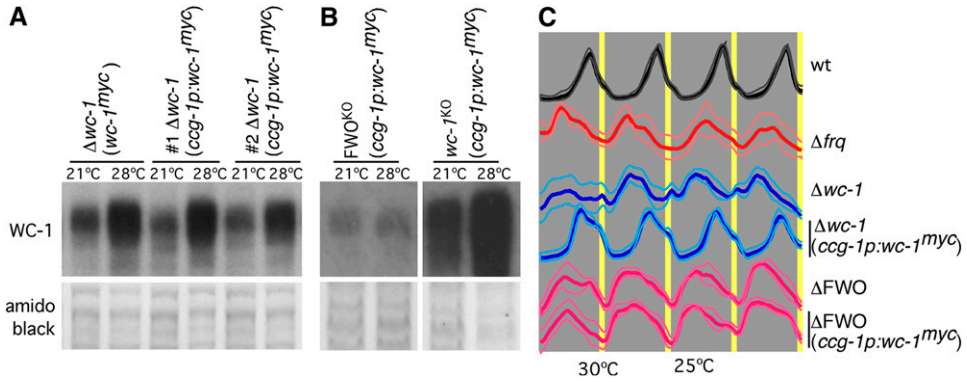

Figure 6 A functional WCC is required to rescue the temperature-entrained FLO. (A) Transgenic Δ*wc-1* strains at 21° and 28° in which *wc-1*^{myc} expression is driven from the *wc-1* (*wc-1*^{myc}) or the *ccg-1* promoter (*ccg-1*p:*wc-1*^{myc}). (B) Transgenic ΔFWO and Δ*wc-1* strains at 21° and 28° with *wc-1*^{myc} expression driven from the *ccg-1* promoter (*ccg-1*p:*wc-1*^{myc}). The amido black-stained membrane serves as a loading control. (C) Conidial rhythmicity in T24 skeleton temperature cycles of the indicated wild-type, clock-mutant, and transgenic Δ*wc-1* and ΔFWO strains.

relatively normal in a Δ*wc-1* strain (Denault *et al.* 2001) allows for two interpretations with respect to their similar phenotype in temperature T cycles; *i.e.*, either WC-1 alone or the WCC are essential for establishing the FLO. To test whether WC-1 alone is sufficient to establish a FLO, we decided to overexpress the *wc-1* gene in a ΔFWO strain. Because *wc-1* expression is self-regulatory, we used the strongly expressed *ccg-1* promoter to drive high levels of *wc-1* expression, and, to facilitate the detection of WC-1 in transgenic strains, we used constructs that expressed WC-1 that was Myc-tagged at the N terminus. As can be seen in Figure 6A, the use of a *ccg-1*-driven *wc-1* construct does lead to similar WC-1 levels when compared to those seen in strains in which *wc-1* is driven by its own promoter. Targeted integration of the *ccg-1:wc-1*^{myc} construct at *his-3* rescues rhythmicity in a Δ*wc-1* strain at 25° and 28°, with a period and phase similar, albeit not identical, to that of wild type (see Figure 6C), indicating that the tagged WC-1 protein is functional. Next, we decided to see if the *ccg-1:wc-1*^{myc} construct could rescue the FLO in ΔFWO strains in T24 skeleton cycles of 22 hr at 25° and 2 hr at 30°. As can be seen in Figure 6C, expression of WC-1 in a ΔFWO strain does not lead to any significant change in overt rhythmicity. Despite the use of the *ccg-1* promoter, levels of ectopically expressed WC-1 are significantly lower in a ΔFWO strain when compared to the same construct expressed in a Δ*wc-1* single knockout (compare left and right in Figure 6B). This observation is consistent with previous results that have shown that complex formation with WC-2 is critical for WC-1 stability (Cheng *et al.* 2002) and that FRQ is involved in stabilizing WC-1 levels (Lee *et al.* 2000; Schafmeier *et al.* 2008). While possible, we consider it unlikely that levels of WC-1 are too low to drive the FLO because WC-1 levels in a Δ*frq* (where the FLO is present) are similarly low (Lee *et al.* 2000). Taken together, these results show that WC-1 alone is not sufficient for the FLO and that a functional WCC is required to rescue the temperature-entrained FLO.

We have shown here that, in symmetrical temperature cycles, rhythmic conidiation of a ΔFWO strain that lacks both *frq* and *wc* genes resembles, and can be modeled as, an hourglass-type response to temperature. While the FLO seen in Δ*frq* strains bestowed a residual ability to restrict spore development to certain times during the cold period, this was not the case in a ΔFWO strain. In fact, deletion of either *wc-1* or *wc-2* leaves little evidence of a FLO, and a ΔFWO strain lacks any such evidence. Our data suggest that the WCC is crucial for this inhibitory activity and imparts the properties of a FLO on a *frq*-less strain. In stark contrast, rhythmicity in strains that are wild type for the circadian FWO displayed hallmarks of entrainment. Importantly, the phases of the entrained FWO were accurately predicted from our PRC-based model. In summary, by ablating the *frq* and, subsequently, the *wc* genes, temperature-entrained rhythms in spore development can be gradually transformed from a clock-controlled process to a simple stimulus response via a transitional state that is controlled by the FLO. Our data help to reconcile some of the conflicting views on the nature of the FLO, views that were mostly based on an analysis of the timing of conidiation in *frq*-less strains. As we have seen, repression of conidiation is largely dependent on a functional WCC. Levels of WC-1, albeit strongly reduced in *frq*-less strains (Lee *et al.* 2000), are clearly detectable and must still be able to actively suppress conidiation. Since WC-1 and WC-2 levels are temperature-controlled (Suzanne Hunt, unpublished results, and Figure 6A), it is conceivable that the time of conidial suppression is temperature-dependent and, within limits, may have an effect on controlling spore development in a Δ*frq* strain. Recently, de Paula *et al.* (2006, 2007) proposed a model in which a WC-FLO acts in conjunction with the classical FWO to provide robust entrainment to light and temperature cues. In analogy to the coupled morning (M) and evening (E) oscillators that were first proposed to control eclosion rhythms in *Drosophila* (Pittendrigh and Bruce 1959) and similar multi-oscillator loops predicted to act within the plant and mammalian circadian clocks (Leloup and Goldbeter 2004; Locke *et al.* 2006), the authors speculate that the WCC couples both the classic FWO (M-Oscillator) and the WC-FLO (E-Oscillator) to provide robust entrainment to light and temperature cues. While our study did not test this hypothesis, our data are consistent with the proposed multi-oscillator model. This aside, our data show further support for WCC as a central component for creating temperature-induced oscillatory behavior in the absence of the FWO. Because similar phenomena have been observed in other eukaryotic model organisms when lacking their respective circadian core components, the

study of oscillatory phenomena that center on the *Neurospora* WCC promises to provide general insights into the molecular organization of circadian systems.

Acknowledgments

We thank Sue Crosthwaite (University of Manchester) for helpful suggestions and critical reading of the manuscript. This work was supported by grants from the Biotechnology and Biological Sciences Research Council to C.H. (BB/D00988X/1 and BB/F012055/1).

Literature Cited

Aronson, B. D., K. A. Johnson, and J. C. Dunlap, 1994 Circadian clock locus *frequency*: protein encoded by a single open reading frame defines period length and temperature compensation. Proc. Natl. Acad. Sci. USA 91: 7683–7687.

Belden, W. J., L. F. Larrondo, A. C. Froehlich, M. Shi, C. H. Chen *et al.*, 2007 The *band* mutation in *Neurospora crassa* is a dominant allele of ras-1 implicating RAS signaling in circadian output. Genes Dev. 21: 1494–1505.

Bell-Pedersen, D., V. M. Cassone, D. J. Earnest, S. S. Golden, P. E. Hardin *et al.*, 2005 Circadian rhythms from multiple oscillators: lessons from diverse organisms. Nat. Rev. Genet. 6: 544–556.

Bieszke, J. A., E. L. Braun, L. E. Bean, S. Kang, D. O. Natvig *et al.*, 1999 The nop-1 gene of *Neurospora crassa* encodes a seven transmembrane helix retinal-binding protein homologous to archaeal rhodopsins. Proc. Natl. Acad. Sci. USA 96: 8034–8039.

Bruce, V. G., 1960 Environmental entrainment of circadian rhythms. Cold Spring Harb. Symp. Quant. Biol. 25: 29–48.

Cheng, P., Y. H. Yang, K. H. Gardner, and Y. Liu, 2002 PAS domain-mediated WC-1/WC-2 interaction is essential for maintaining the steady-state level of WC-1 and the function of both proteins in circadian clock and light responses of Neurospora. Mol. Cell. Biol. 22: 517–524.

Christensen, M. K., G. Falkeid, J. J. Loros, J. C. Dunlap, C. Lillo *et al.*, 2004 A nitrate-induced *frq*-less oscillator in *Neurospora crassa*. J. Biol. Rhythms 19: 280–286.

Collett, M. A., N. Garceau, J. C. Dunlap, and J. J. Loros, 2002 Light and clock expression of the Neurospora clock gene frequency is differentially driven by but dependent on WHITE COLLAR-2. Genetics 160: 149–158.

Correa, A., A. Z. Lewis, A. V. Greene, I. J. March, R. H. Gomer *et al.*, 2003 Multiple oscillators regulate circadian gene expression in Neurospora. Proc. Natl. Acad. Sci. USA 100: 13597–13602.

Crosthwaite, S. K., J. C. Dunlap, and J. J. Loros, 1997 Neurospora *wc-1* and *wc-2*: transcription, photoresponses, and the origins of circadian rhythmicity. Science 276: 763–769.

Denault, D. L., J. J. Loros, and J. C. Dunlap, 2001 WC-2 mediates WC-1-FRQ interaction within the PAS protein-linked circadian feedback loop of Neurospora. EMBO J. 20: 109–117.

de Paula, R. M., Z. A. Lewis, A. V. Greene, K. S. Seo, L. W. Morgan *et al.*, 2006 Two circadian timing circuits in *Neurospora crassa*. J. Biol. Rhythms 21: 159–168.

de Paula, R. M., M. W. Vitalini, R. H. Gomer, and D. Bell-Pedersen, 2007 Complexity of the *Neurospora crassa* circadian clock system: multiple loops and oscillators. Cold Spring Harb. Symp. Quant. Biol. 72: 345–351.

Dharmananda, S., 1980 Studies of the circadian clock of *Neurospora crassa* light-induced phase shifting. Ph.D. Thesis, University of California, Santa Cruz.

Dodd, A. N., N. Salathia, A. Hall, E. Kevei, R. Toth *et al.*, 2005 Plant circadian clocks increase photosynthesis, growth, survival, and competitive advantage. Science 309: 630–633.

Dunlap, J. C., 1999 Molecular bases for circadian clocks. Cell 96: 271–290.

Elvin, M., J. J. Loros, J. C. Dunlap, and C. Heintzen, 2005 The PAS/LOV protein VIVID supports a rapidly dampened daytime oscillator that facilitates entrainment of the Neurospora circadian clock. Genes Dev. 19: 2593–2605.

Freitag, M., P. C. Hickey, N. B. Raju, E. U. Selker, and N. D. Read, 2004 GFP as a tool to analyze the organization, dynamics and function of nuclei and microtubules in Neurospora crassa. Fungal Genet. Biol. 41: 897–910.

Froehlich, A. C., B. Noh, R. D. Vierstra, J. Loros, and J. C. Dunlap, 2005 Genetic and molecular analysis of phytochromes from the filamentous fungus *Neurospora crassa*. Eukaryot. Cell 4: 2140–2152.

Froehlich, A. C., C. H. Chen, W. J. Belden, C. Madeti, T. Roenneberg *et al.*, 2010 Genetic and molecular characterization of a cryptochrome from the filamentous fungus *Neurospora crassa*. Eukaryot. Cell 9: 738–750.

Garceau, N. Y., Y. Liu, J. J. Loros, and J. C. Dunlap, 1997 Alternative initiation of translation and time-specific phosphorylation yield multiple forms of the essential clock protein FREQUENCY. Cell 89: 469–476.

Granshaw, T., M. Tsukamoto, and S. Brody, 2003 Circadian rhythms in *Neurospora crassa*: farnesol or geraniol allow expression of rhythmicity in the otherwise arrhythmic strains *frq*(10), *wc-1*, and *wc-2*. J. Biol. Rhythms 18: 287–296.

Hansberg, W., H. de Groot, and H. Sies, 1993 Reactive oxygen species associated with cell differentiation in *Neurospora crass*a. Free Radic. Biol. Med. 14: 287–293.

He, Q., P. Cheng, Q. He, and Y. Liu, 2005 The COP9 signalosome regulates the Neurospora circadian clock by controlling the stability of the SCFFWD-1 complex. Genes Dev. 19: 1518–1531.

Heintzen, C., and Y. Liu, 2007 The *Neurospora crassa* circadian clock. Adv. Genet. 58: 25–66.

Heintzen, C., J. J. Loros, and J. C. Dunlap, 2001 The PAS protein VIVID defines a clock-associated feedback loop that represses light input, modulates gating, and regulates clock resetting. Cell 104: 453–464.

Hunt, S. M., M. Elvin, S. K. Crosthwaite, and C. Heintzen, 2007 The PAS/LOV protein VIVID controls temperature compensation of circadian clock phase and development in *Neurospora crassa*. Genes Dev. 21: 1964–1974.

Iwasaki, H., and J. C. Dunlap, 2000 Microbial circadian oscillatory systems in Neurospora and Synechococcus: models for cellular clocks. Curr. Opin. Microbiol. 3: 189–196.

Johnson, C. H., J. A. Elliott, and R. Foster, 2003 Entrainment of circadian programs. Chronobiol. Int. 20: 741–774.

Johnson, C. H., J. Elliott, R. Foster, K. Honma, and R. E. Kronauer, 2004 Fundamental properties of circadian rhythms, pp. 67–105 in *Chronobiology*, edited by J. Dunlap, J. Loros, and P. J. DeCoursey. Sinauer Associates, Sunderland, MA.

Lakin-Thomas, P. L., 1998 Choline depletion, *frq* mutations, and temperature compensation of the circadian rhythm in *Neurospora crassa*. J. Biol. Rhythms 13: 268–277.

Lakin-Thomas, P. L., 2006 Circadian clock genes frequency and white collar-1 are not essential for entrainment to temperature cycles in *Neurospora crassa*. Proc. Natl. Acad. Sci. USA 103: 4469–4474.

Lakin-Thomas, P. L., and S. Brody, 2000 Circadian rhythms in *Neurospora crassa* lipid deficiencies restore robust rhythmicity to null frequency and white-collar mutants. Proc. Natl. Acad. Sci. USA 97: 256–261.

Lakin-Thomas, P. L., and S. Brody, 2004 Circadian rhythms in microorganisms: new complexities. Annu. Rev. Microbiol. 58: 489–519.

Lee, K., J. J. Loros, and J. C. Dunlap, 2000 Interconnected feedback loops in the Neurospora circadian system. Science 289: 107–110.

Lee, K., J. C. Dunlap, and J. J. Loros, 2003 Roles for WHITE COLLAR-1 in circadian and general photoperception in *Neurospora crassa*. Genetics 163: 103–114.

Leloup, J. C., and A. Goldbeter, 2004 Modeling the mammalian circadian clock: sensitivity analysis and multiplicity of oscillatory mechanisms. J. Theor. Biol. 230: 541–562.

Li, S., and P. Lakin-Thomas, 2010 Effects of prd circadian clock mutations on FRQ-less rhythms in Neurospora. J. Biol. Rhythms 25: 71–80.

Locke, J. C., L. Kozma-Bognar, P. D. Gould, B. Feher, E. Kevei *et al.*, 2006 Experimental validation of a predicted feedback loop in the multi-oscillator clock of Arabidopsis thaliana. Mol. Syst. Biol. 2: 59.

Loros, J. J., and J. F. Feldman, 1986 Loss of temperature compensation of circadian period length in the *frq-9* mutant of *Neurospora crassa*. J. Biol. Rhythms 1: 187–198.

Loros, J. J., A. Richman, and J. F. Feldman, 1986 A recessive circadian clock mutation at the *frq* locus of *Neurospora crassa*. Genetics 114: 1095–1110.

Loros, J. J., J. C. Dunlap, L. F. Larrondo, M. Shi, W. J. Belden *et al.*, 2007 Circadian output, input, and intracellular oscillators: insights into the circadian systems of single cells. Cold Spring Harb. Symp. Quant. Biol. 72: 201–214.

Merrow, M., and T. Roenneberg, 2007 Circadian entrainment of *Neurospora crassa*. Cold Spring Harb. Symp. Quant. Biol. 72: 279–285.

Merrow, M., M. Brunner, and T. Roenneberg, 1999 Assignment of circadian function for the Neurospora clock gene frequency. Nature 399: 584–586.

Olmedo, M., C. Ruger-Herreros, E. M. Luque, and L. M. Corrochano, 2010 A complex photoreceptor system mediates the regulation by light of the conidiation genes con-10 and con-6 in *Neurospora crassa*. Fungal Genet. Biol. 47: 352–363.

Ouyang, Y., C. R. Andersson, T. Kondo, S. S. Golden, and C. H. Johnson, 1998 Resonating circadian clocks enhance fitness in cyanobacteria. Proc. Natl. Acad. Sci. USA 95: 8660–8664.

Pittendrigh, C., and V. Bruce, 1959 Daily rhythms as coupled oscillator systems and their relation to thermoperiodism and photoperiodism, pp. 475–505 in *Photoperiodism and Related Phenomena in Plants and Animals*, edited by R. B. Withrow. American Association for the Advancement of Science, Washington, DC.

Pregueiro, A. M., N. Price-Lloyd, D. Bell-Pedersen, C. Heintzen, J. J. Loros *et al.*, 2005 Assignment of an essential role for the Neurospora frequency gene in circadian entrainment to temperature cycles. Proc. Natl. Acad. Sci. USA 102: 2210–2215.

Price-Lloyd, N., M. Elvin, and C. Heintzen, 2005 Synchronizing the *Neurospora crassa* circadian clock with the rhythmic environment. Biochem. Soc. Trans. 33: 949–952.

Roenneberg, T., and M. Merrow, 2001 Circadian systems: different levels of complexity. Philos. Trans. R. Soc. Lond. B Biol. Sci. 356: 1687–1696.

Roenneberg, T., and W. Taylor, 2000 Automated recordings of bioluminescence with special reference to the analysis of circadian rhythms. Methods Enzymol. 305: 104–119.

Roenneberg, T., S. Daan, and M. Merrow, 2003 The art of entrainment. J. Biol. Rhythms 18: 183–194.

Roenneberg, T., Z. Dragovic, and M. Merrow, 2005 Demasking biological oscillators: properties and principles of entrainment exemplified by the Neurospora circadian clock. Proc. Natl. Acad. Sci. USA 102: 7742–7747.

Schafmeier, T., A. Diernfellner, A. Schafer, O. Dintsis, A. Neiss *et al.*, 2008 Circadian activity and abundance rhythms of the Neurospora clock transcription factor WCC associated with rapid nucleo-cytoplasmic shuttling. Genes Dev. 22: 3397–3402.

Schmoll, M., L. Franchi, and C. P. Kubicek, 2005 Envoy, a PAS/LOV domain protein of *Hypocrea jecorina* (Anamorph *Trichoderma reesei*), modulates cellulase gene transcription in response to light. Eukaryot. Cell 4: 1998–2007.

Schneider, K., S. Perrino, K. Oelhafen, S. Li, A. Zatsepin *et al.*, 2009 Rhythmic conidiation in constant light in vivid mutants of *Neurospora crassa*. Genetics 181: 917–931.

Yoshida, Y., and K. Hasunuma, 2004 Reactive oxygen species affect photomorphogenesis in *Neurospora crassa*. J. Biol. Chem. 279: 6986–6993.

Communicating editor: E. U. Selker

GENETICS

Supporting Information
http://www.genetics.org/content/suppl/2012/02/23/genetics.111.137976.DC1

Temperature-Sensitive and Circadian Oscillators of *Neurospora crassa* Share Components

Suzanne Hunt, Mark Elvin, and Christian Heintzen

DOI: 10.1534/genetics.111.137976

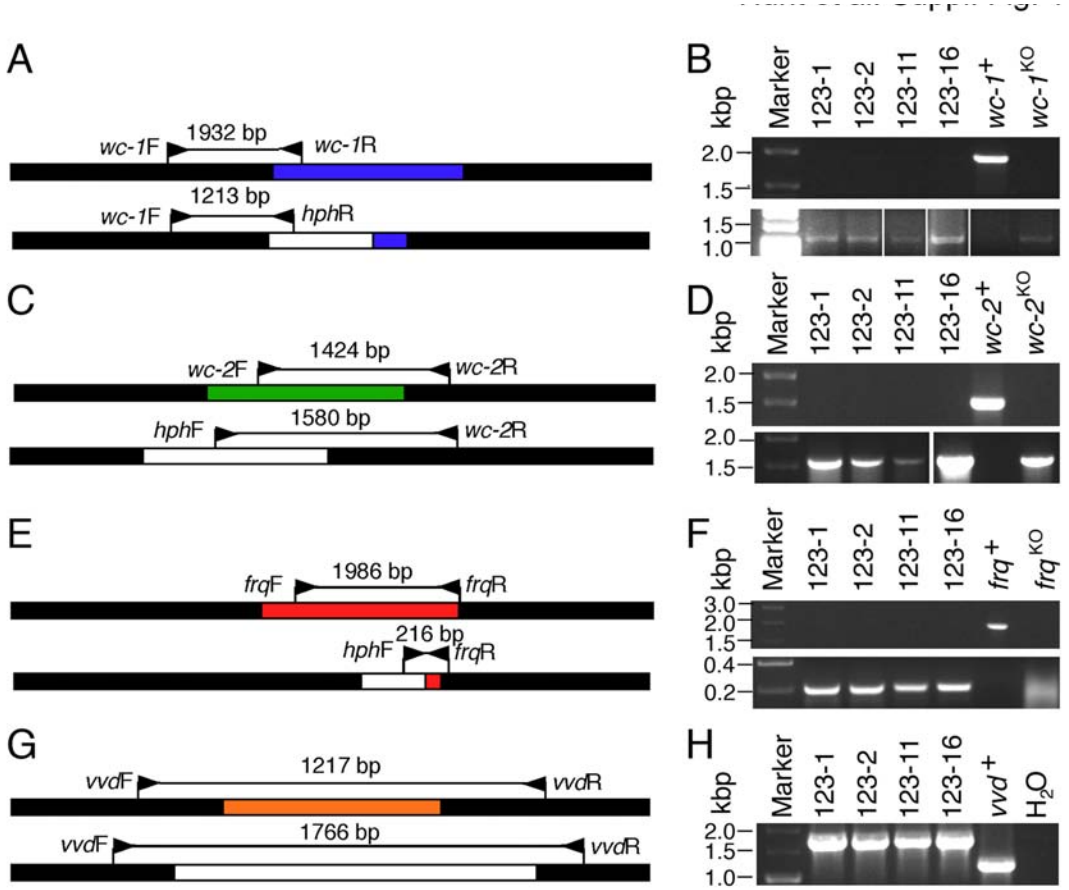

Figure S1 Verification of ΔFWO strains by genomic PCR. (A) Schematic illustration of the *wc-1*$^{+}$ and Δ*wc-1* loci showing position of primers used in B and the expected sizes of PCR products. (B). PCR amplification products of *wc-1* loci using genomic DNA from *wc-1*$^{+}$ and Δ*wc-1* control strains and four putative ΔFWO strains (123-1, 123-2, 123-11, 123-12) as a template and *wc-1*F and *wc-1*R (top panel) or *wc-1*F and *hph*R (Bottom panel) as amplification primers. (C) Schematic illustration of the *wc-2*$^{+}$ and Δ*wc-2* loci showing position of primers used in D and expected sizes of PCR products. (D). PCR amplification products using a strategy analogous to that shown in B. (E) Schematic illustration of the *frq*$^{+}$ and Δ*frq* loci showing position of primers used in F and expected sizes of PCR products. (F). PCR amplification products using a strategy analogous to that shown in B. (G) Schematic illustration of the *vvd*$^{+}$ and *Δvvd* loci showing position of primers used in H and expected sizes of PCR products. (H). PCR amplification products using the primers shown in G. H_2O = negative control.

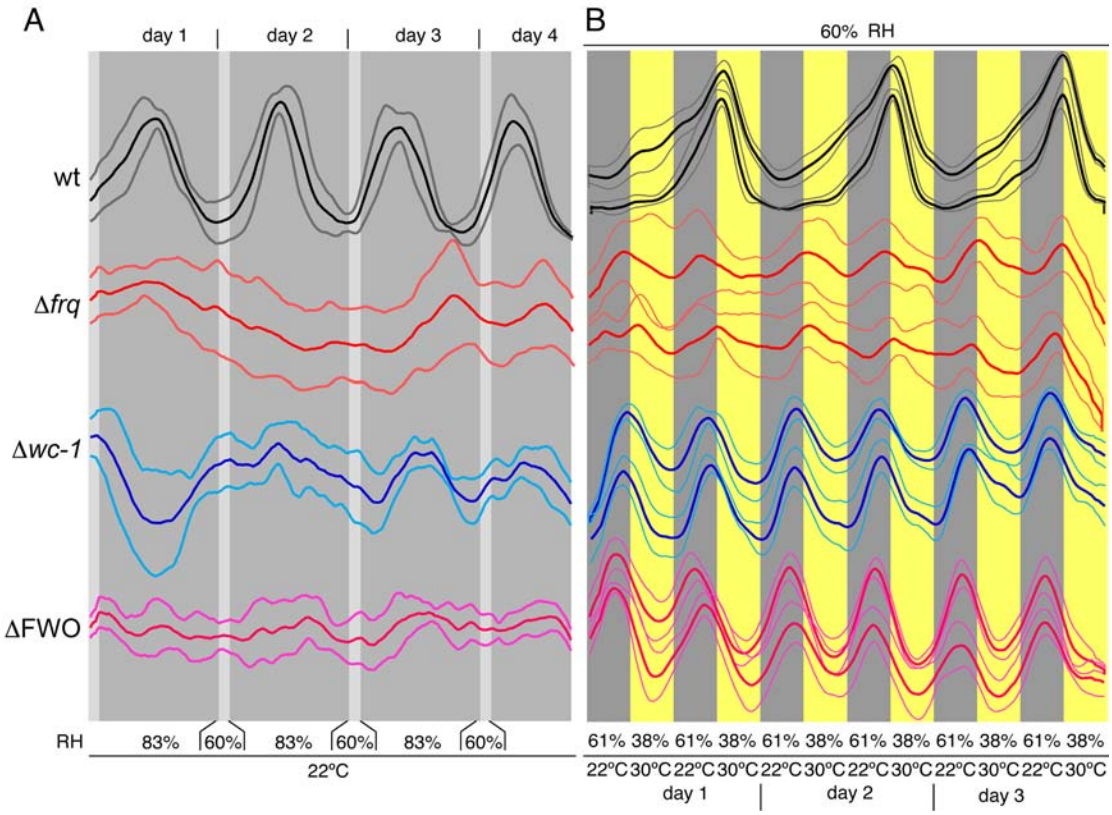

Figure S2 Changes in relative humidity do not influence rhythms in conidiation in Neurospora. (A) Race tube cultures were kept in DD at 22°C and exposed to a T24 skeleton humidity T-cycle consisting of 2h at 60% relative humidity (RH) and 22h at 83% RH. The period of the WT rhythm is 22.4 h +/- 0.26 h (n=6). (B) Strains were grown on race tubes in complete temperature T12 cycles (6h @ 22°C, 6h @ 30°C) at a constant relative humidity (RH) of 60% (top traces for each strain) or without humidity control (bottom traces for each strain), i.e. the temperature change led to corresponding changes in RH between 61% RH at 22°C and 38% RH at 30°C. Thick lines = mean, thin lines = +/- 1 standard deviation, (n=6).

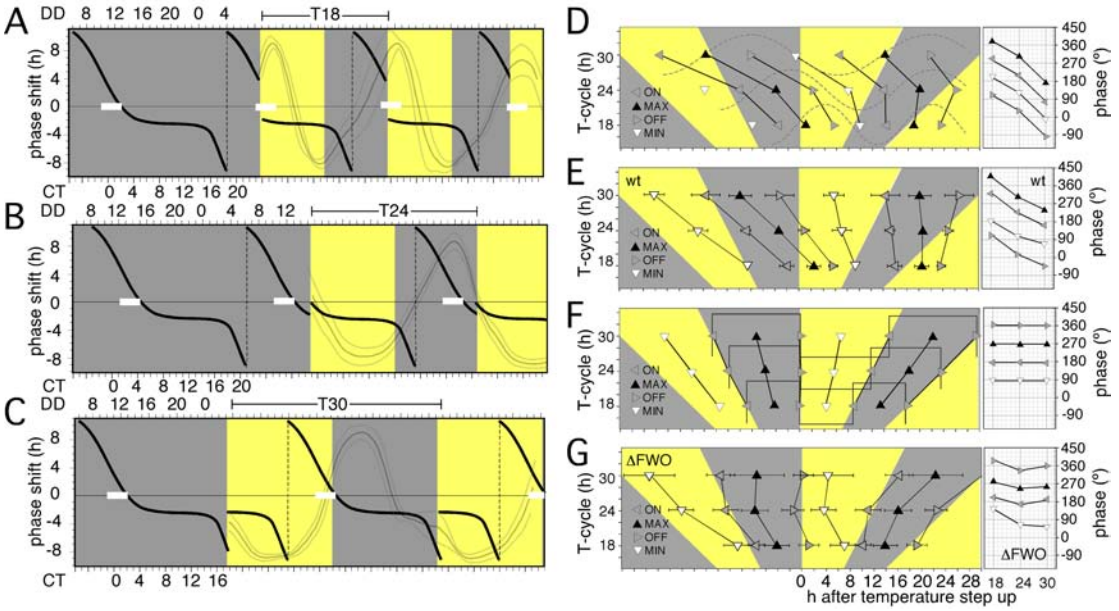

Figure S3 Predicting the position of phase markers of entrained and hourglass-type rhythms in Neurospora wild type and circadian clock-mutants in complete temperature T-cycles. (A-C) The Neurospora phase response curve (PRC, black) to 2h temperature pulses of 30°C as explained in Fig 5A-D was used to predict entrainment of Neurospora wild type to complete temperature cycles. (D,E) Simulated (D) and experimental position (E) of phase markers of conidial rhythms entrained to T-cycles shown. Conidial rhythms were simulated by simple sine waves and the predicted phase markers are based on the PRC introduced above. Experimental data are derived from phase analysis of race tube data shown in Fig. 4A. The phase markers are recorded in hours following the start of the temperature pulse (yellow) and are onsets (ON), offsets (OFF), peaks (MAX) and troughs (MIN) of conidiation. The graphs on the right depict the dependence of phase (expressed in degrees) on T-cycle. For experimental data, only the mean phases are shown. (F) Simulated hourglass-type behaviour and (G) experimental data for the ΔFWO strain. The rhythm has a rectangular waveform, reflecting a simple stimulus response with conidiation activated throughout the cold phase and repressed throughout the warm phase. In this scenario on and offsets of conidiation coincide with the temperature transitions, whilst the peaks and troughs are ill defined and arbitrarily set to the middle of the cold and warm phases respectively. Phase markers and graph are as described above.

Table S1 Neurospora strains

Strain names	Genotypes	Shorthand notation used in this study	Source
87-3	*ras-1^{bd}, a*		Laboratory stock
87-12	*ras-1^{bd}; A*		Laboratory stock
54-3	*ras-1^{bd}, a*	Wild type (wt)	Laboratory stock
86-1	*his-3; ras-1^{bd},* Δ*frq; A*		Aronson et al., 1994
54-6	*his-3; ras-1^{bd},* Δ*frq; A*	Δ*frq*	Laboratory stock (87-3 x 86-1)
54-11	*ras-1^{bd};* Δ*frq; a*		This study (87-3 x 86-1)
308-1	*his-3; ras-1^{bd},* Δ*wc-1; a*		Lee et al., 2003
104-2	*his-3; ras-1^{bd},* Δ*wc-1; A*		Laboratory stock (87-12 x 308-1)
104-104	*ras-1^{bd};* Δ*wc-1; a*	Δ*wc-1*	This study (87-12 x 308-1)
241-23	*his-3* Δ*wc-2; ras-1^{bd}; A*		Collett et al., 2002
55-3	*his-3* Δ*wc-2; ras-1^{bd}; A*		Laboratory stock (87-3 x 241-23)
50-1	Δ*wc-2; ras-1^{bd}; a*	Δ*wc-2*	This study (87-3 x 241-23)
289-10	*his-3; ras-1^{bd};* Δ*vvd; A*		Elvin et al., 2005
56-7	*ras-1^{bd};* Δ*vvd; a*	Δ*vvd*	This study (87-3 x 289-10)
102-5	*ras-1^{bd};* Δ*vvd;* Δ*frq; a*		Laboratory stock (54-6 x 56-7)
107-10	*his-3* Δ*wc-2, ras-1^{bd};* Δ*vvd; A*		Laboratory stock (54-3 x 56-7)
108-77	*his-3; ras-1^{bd};* Δ*vvd;* Δ*frq,* Δ*wc-1; A*		Laboratory stock (104-2 x 102-5)
123-2	Δ*wc-2; ras-1^{bd};* Δ*vvd;* Δ*frq,* Δ*wc-1; a*	ΔFWO	This study (107-10 x 108-77)
127-11	*his-3;* Δ*wc-2; ras-1^{bd};* Δ*vvd;* Δ*frq,* Δ*wc-1; A*		Laboratory stock (123-2 x 108-77)
154-1-3	*his-3 (his-3^{+} pSHccg1:WC-1myc);* Δ*wc-2; ras-1^{bd};* Δ*vvd;* Δ*frq,* Δ*wc-1; A*	ΔFWO (*wc-1^{myc}*)	This study: (SHccg1:WC-1myc in 127-11)
154-5-3	*his-3 (his-3^{+} pSHccg1:WC-1myc);* Δ*wc-2; ras-1^{bd};* Δ*vvd;* Δ*frq,* Δ*wc-1; A*	ΔFWO (*ccg-1p:wc-1^{myc}*)	This study: (pSHccg1:WC-1myc in 127-11)
110-12A	*his-3 (his-3^{+}pMyc-WC-1); ras-1^{bd},* Δ*wc-1; A*	Δ*wc-1* (*wc-1^{myc}*)	This study: (pMyc-WC-1 (Cheng et al., 2002) in 104-2)
155-4-3	*his-3 (his-3^{+} pSHccg1:WC-1myc);* Δ*wc-1; A*	Δ*wc-1* (*ccg-1p:wc-1^{myc}*)	This study: (pSHccg1:WC-1myc in 104-2)

Table S2 Values of MAX and MIN phases, standard deviation (SD), sample size (N) and statistical analysis (paired t-test) of phase differences LL and DD conditions for the indicated strains and T-cycles

strain	T-cycle	MAX phase in DD	SD	N	MAX phase in LL	SD	N	MIN phase in DD	SD	N	MIN phase in LL	SD	N	Δphase MAX	t	P	Δphase MIN	t	P
Δfrq	T12	11.6	1.7	38	7.9	1.95	48	5.2	1.6	46	13.6	1.04	48	3.7	9.2404	<0.0001	8.4	30.346	<0.0001
Δfrq	T16	ND	ND	ND	ND	ND	ND	ND	ND	ND	ND	ND	ND	ND	ND	ND	ND	ND	ND
Δfrq	T20	16	2.14	20	9.6	1.17	12	5.4	2.56	24	4.1	1.85	16	6.4	9.5021	<0.0001	1.3	1.7467	0.0888
Δfrq	T24	13.2	2.12	20	8.3	1.08	22	1.2	2.8	17	2.9	1.03	14	4.9	9.5687	<0.0001	1.7	2.1497	0.0401
Δfrq	T28	14.1	1.14	23	10.7	2.1	8	33.1	0.89	17	25	3.07	7	3.4	7.1651	<0.0001	8.1	7.6574	<0.0001
														18.4			**19.5**		
Δwc-1	T12	10.9	2.37	45	12.6	1.3	40	3.3	0.84	43	5.1	1.02	35	1.7	4.0281	<0.0001	1.8	8.549	<0.0001
Δwc-1	T16	11.2	2.17	17	7.6	2	23	4.7	0.82	12	2	0.7	13	(3.6)*	5.4288	<0.0001	(2.7)*	8.8773	<0.0001
Δwc-1	T20	17.1	2.11	12	13	1.29	18	22.8	2.31	12	24.1	1.58	20	4.1	6.6228	<0.0001	1.3	1.8929	0.0681
Δwc-1	T24	13	1.5	16	11.7	2.17	17	3.4	1.47	12	2.1	2.31	15	1.3	1.9895	0.0555	1.3	1.6912	0.1032
Δwc-1	T28	16.3	2.74	15	18.8	2.81	20	27.7	1.98	14	32.9	1.13	10	2.5	2.6323	0.0128	**5.2**	7.4539	<0.0001
														9.6			**9.6**		
ΔFWO	T12	8.9	1.28	30	8.9	1.25	41	2.4	1.02	30	2.8	0.84	41	0	0	1	0.4	1.8097	0.0747
ΔFWO	T16	10.4	1.45	32	7.3	1.74	34	2.2	0.7	35	2.3	0.66	30	(3.1)*	7.8368	<0.0001	(0.1)*	0.5894	0.5577
ΔFWO	T20	14.4	1.68	15	10.2	1.81	30	4.4	1.45	14	3	0.62	24	4.2	7.5091	0.0128	1.4	4.153	0.0002
ΔFWO	T24	14.3	1.08	22	14.2	1.64	24	1.8	0.56	18	2.9	0.82	18	0.1	0.2418	0.81	1.1	4.6999	<0.0001
ΔFWO	T28	14.1	1.67	24	15.5	2.5	24	2.4	1.88	23	3.7	1.01	18	1.4	2.2813	0.0272	1.3	2.6454	0.0117
														5.7			**4.2**		

* phase data in brackets were not used for obtaining the sum of the phase differences as they could not be determined for the Δ*frq* strain